Synthesis, characterization and photoluminescence of 8-oxyquinolinato organoboron complexes derived from pyrazole

Krzysztof Durka, Agnieszka Górska, Piotr Jankowski, Tomasz Kliś, Marcin Kublicki, Janusz Serwatowski, Mateusz Urban, Grzegorz Wesela-Bauman, Krzysztof Woźniak

PII: S0040-4039(17)30193-4
DOI: http://dx.doi.org/10.1016/j.tetlet.2017.02.022
Reference: TETL 48633

To appear in: *Tetrahedron Letters*

Received Date: 28 November 2016
Revised Date: 4 February 2017
Accepted Date: 8 February 2017

Please cite this article as: Durka, K., Górska, A., Jankowski, P., Kliś, T., Kublicki, M., Serwatowski, J., Urban, M., Wesela-Bauman, G., Woźniak, K., Synthesis, characterization and photoluminescence of 8-oxyquinolinato organoboron complexes derived from pyrazole, *Tetrahedron Letters* (2017), doi: http://dx.doi.org/10.1016/j.tetlet.2017.02.022

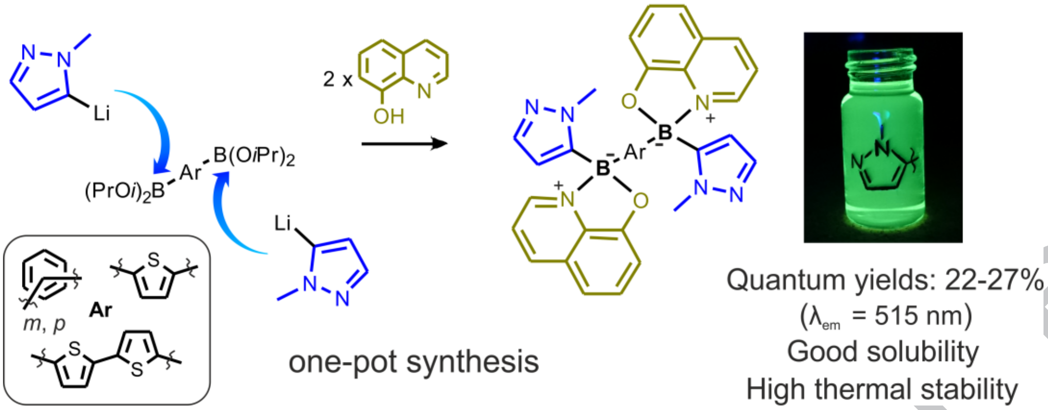
N
N
Li
(PrO*i*)$_2$B
Ar
B(O*i*Pr)$_2$
Li
N
N
2 x
N
OH
Ar
m, *p*
S
S
S
one-pot synthesis
N
N
O
N
B
Ar
B
N
O
N
N
Quantum yields: 22-27%
(λ$_{em}$ = 515 nm)
Good solubility
High thermal stability

Synthesis, characterization and photoluminescence of 8-oxyquinolinato organoboron complexes derived from pyrazole

Krzysztof Durka[†], Agnieszka Górska[†], Piotr Jankowski[†], Tomasz Kliś[†*], Marcin Kublicki[†], Janusz Serwatowski[†], Mateusz Urban[†], Grzegorz Wesela-Bauman[†], Krzysztof Woźniak[‡]

†*Warsaw University of Technology, Faculty of Chemistry, Noakowskiego 3, 00-664 Warsaw, Poland*

‡*Warsaw University, Faculty of Chemistry, Pasteura 1, 02-093 Warsaw, Poland*

Abstract

A one-pot protocol was developed for the synthesis of a series of luminescent heteroleptic diaryldiborinic complexes containing the central aryl ring bonded to two boron atoms substituted with pyrazole and complexed with 8-hydroxyquinoline. The luminescent properties of these compounds were measured. In dilute solutions they exhibited an emission at *c.a.* 513 nm with quantum yields of 22-27% which are typical for borinic 8-hydroxyquinoline complexes. The only exception was the complex containing the bithiophene scaffold, for which no fluorescence was observed. The obtained pyrazole-based complexes show improved solubility and thermal stability with respect to their phenyl analogues. The experimental UV-vis absorption and emission data are supported by theoretical calculations of the frontier molecular orbitals, revealing the aromatic linker to quinolinato ligand excitation mechanism.

Keywords: pyrazole, lithiation, quinoline, borates, luminescence

Introduction

Amongst reported borinic complexes with various chelating ligands, heteroleptic diarylboron derivatives are promising luminescent materials in organic light-emitting devices (OLEDs),[1-18] due to their high stability and good emission properties. A recent study by our research group reported a synthetic approach to a novel class of fluorescent diarylborinic 8-oxyquinolinates RR'BQ (Q – quinolinato ligand) bearing aryl (R) substituents and the pyridine moiety (R'), for which the physicochemical properties were tuned by changing the substituent attached to the boron atom (Scheme 1).[19] Emission maxima ranging from 502 to 525 nm and 10–20% quantum yield were reported for these compounds. The introduction of a second boron atom linked to another oxyquinolinato ligand is a useful tool to influence the optical properties, as previously demonstrated for a series of 9,10-dihydro-9,10-diboraanthracene-bis(8-oxyquinolinates).[20] In such dinuclear

---

[*] Corresponding author. Tel.: +48 22 2347575; fax: +48 22 6282741. E-mail address: ktom@ch.pw.edu.pl

complexes, the quantum yield of emission ranges from 40 to 62% depending on the position of the halogen substituent. We believe there is still a need for diverse modification of the aromatic rings attached to the boron atom in order to further improve the optical properties of the obtained borinic complexes. To the best of our knowledge, no studies concerning the influence of the pyrazole (Pz) ring on the physicochemical properties of such complexes have been performed. Herein, we present the synthesis and physicochemical analysis of a series of heteroleptic diaryldiborinic complexes of the general formula PzB(Q)Ar(Q)BPz (Pz – 1-methyl-1*H*-pyrazole-5-yl, Ar – phenyl or thiophene), i.e. those containing a central aryl ring bonded to two boron atoms substituted with pyrazole and complexed with 8-hydroxyquinoline.

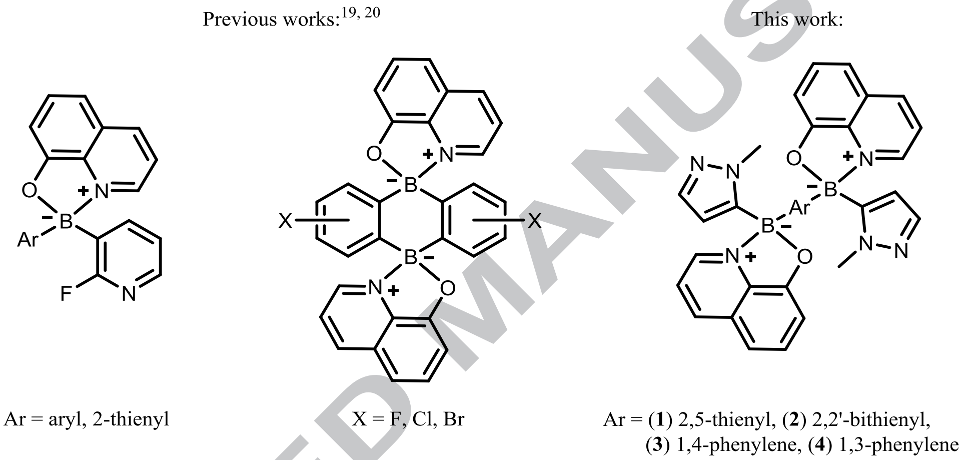
Previous works:[19, 20]

This work:

Ar = aryl, 2-thienyl

X = F, Cl, Br

Ar = (**1**) 2,5-thienyl, (**2**) 2,2'-bithienyl,
(**3**) 1,4-phenylene, (**4**) 1,3-phenylene

Scheme 1. Structures of quinoline boron complexes.

Results and Discussion

The key step in the synthesis of compounds **1-4** involved reaction of the respective diboronic diisopropyl esters **6-9**, which were derived from benzene or thiophene, with lithiated 1-methylpyrazole at -78 °C in THF (Scheme 2). The resultant diaryldiborinic “ate” complexes of the general formula $[Ar]\{[pz]B[O\textit{i}Pr]_2Li\}_2$ were carefully quenched with a Et_2O solution of HCl to give the free diaryldiborinic ester $[Ar]\{[pz]B[O\textit{i}Pr]\}_2$ which were immediately treated with 8-hydroxyquinoline to give the final product as bright yellow or green precipitates. Compound **5** containing two phenyl groups bonded to the boron atoms was synthesized in an analogous manner as a reference compound in order to check the influence of the pyrazole ring on the luminescent properties of the obtained complexes. All complexes were isolated as crystalline solids and were fully characterized by multinuclear ^{1}H, ^{13}C NMR spectroscopy and IR, except **5**, which was only characterized by IR due to its very low solubility. The purity of the obtained compounds was evaluated using CHN elemental analysis. The structural assignments were consistent with the ^{1}H- and ^{13}C NMR spectra described for other boron-oxyquinolinato complexes.[21] The appearance of an IR absorption band at *ca*. 1380 cm^{-1} indicated formation of the B-N bond.[22] In contrast to **5**, pyrazole based luminescent complexes **1-4** showed very good solubility in common organic solvents, which would be beneficial for the construction of potential devices using solution deposition techniques.

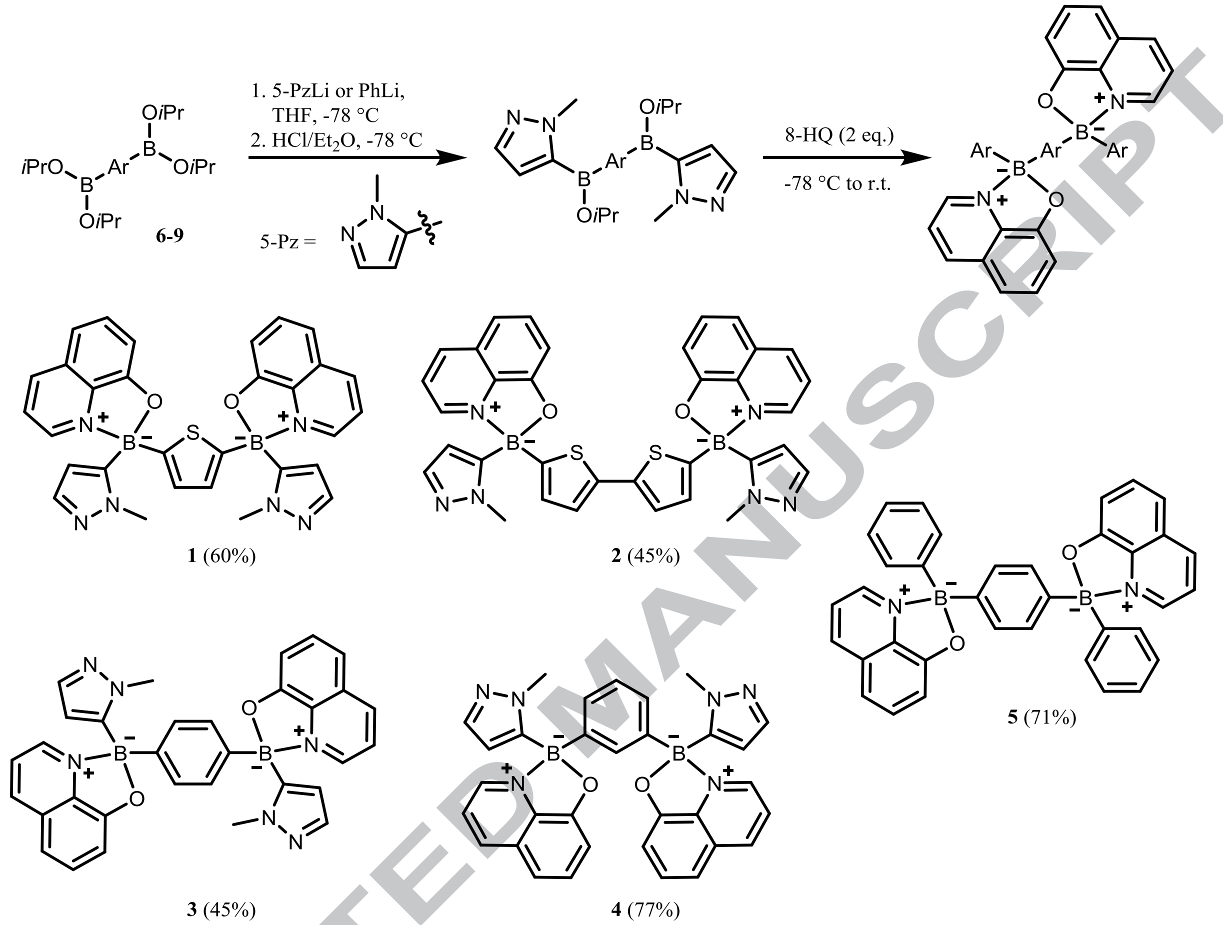

Scheme 2. Synthesis of diaryldiborinic complexes **1**–**5**. Starting materials: **6** – diisopropyl thiophene-2,5-bis-boronate, **7** – diisopropyl bithiophene-2,5-bis-boronate, **8** – diisopropyl phenyl-1,4-bis-boronate, **9** – diisopropyl phenyl-1,3-bis-boronate

The thermal properties of complexes **2-5** were examined by thermogravimetric analysis (TGA) (Fig. S9, ESI). Complex **5** bearing phenyl groups at the boron atoms showed ~5% mass loss when heated to 120 °C, with further gradual loss upon increased temperatures which was also accompanied by slow product decomposition. Substitution with the pyrazole moiety markedly improved the thermal stability, as complexes **3** and **4** began to decompose at 200 °C. These compounds were also more stable than **2**, which may be attributed to the lower stability of the B-C bond in the latter compound.

The formation of complexes **1** and **3** were additionally confirmed by single crystal X-ray diffraction (Fig. 1). The compounds displayed a tetrahedral geometry around the boron centres with B-C, B-O and B-N distances in the ranges typical for other boron oxyquinolinato complexes.[21] Structural analyses revealed that **1** and **3** were formed as *meso* compounds which can adopt either *syn* (**1**) or *anti* (**3**) conformations of the quinolinato moieties with respect to the aromatic ring planes. According to theoretical calculations performed at the M06-2X/6-31++G(d,p)[23] level of theory, both forms were identified as minima on the global potential energy surface, where the *anti* conformation is more stable than the *syn* conformation by 6.0 kJ·mol^{-1} (**1**) and 4.0 kJ·mol^{-1} (**3**). At this point it should be noted that the structural flexibility of the compounds may be reflected by their properties (as charge mobility) in potential photoluminescent devices. The occurrence of two conformers was also observed in solution. In the ^{1}H-NMR spectra of **1**, **3** and **4** two signals at ~3 ppm were observed for the two methyl groups of the pyrazole moieties. This effect was also evident in the ^{13}C-NMR spectra of compounds **1-4** where some resonances were doubled.

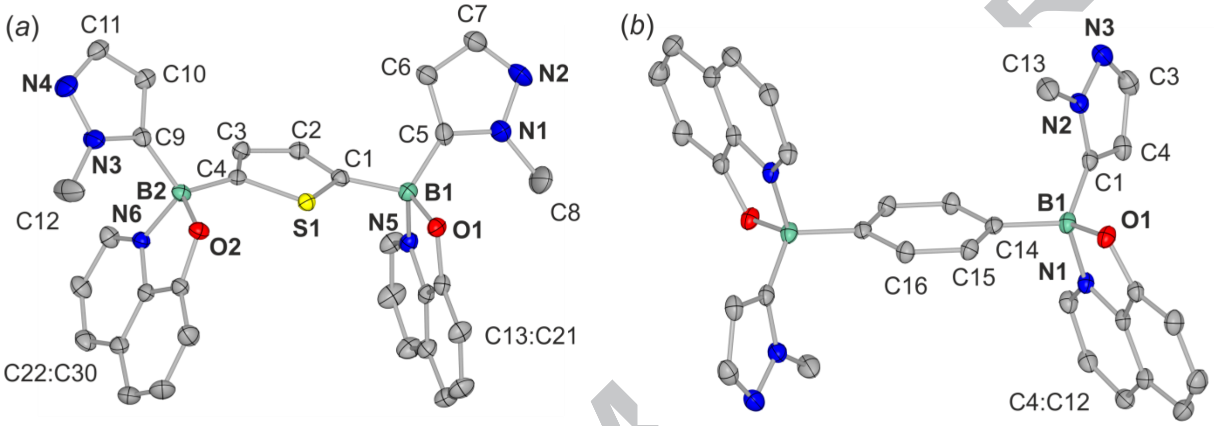

Figure 1. Labelling of atoms and estimation of their atomic thermal motion as ADPs (50% probability level) for **1** (a) and **3** (b).

Absorption and emission spectra of complexes **1-5** recorded in DCM are shown in Fig. 2 (also ESI, Fig S2), and the relevant data compiled in Table 1. Compounds **1** and **2** exhibit two main peaks in their absorption spectra. The longer and less intensive absorption band at ~375–390 nm coincides with the major absorption band of the three remaining complexes. Bithiophene compound **2** exhibits a blue-shift absorption with a relatively high molar extinction coefficient for the higher energy band compared to the monothiophene derivative **1**. In turn, phenyl-bridged analogs **3** and **4** showed practically the same absorption wavelength as the reference compound Ph_2BQ (Table 1).[24] Comparison of the above absorption bands to the value measured for **5** suggests that the nature of the pyrazole substituent did not significantly contribute to the electronic structures of **1-4**.

Emission wavelengths of **1** and **3-5** were practically the same and slightly shifted (by ~10 nm) towards the red region when compared to the reference compound Ph_2BQ (504 nm).[24] The Stokes shifts were also similar for all studied systems and varied in the range of 5800-6300 cm^{-1}, where complexes **1** and **5** represent the largest and smallest values, respectively, from this set. The fluorescence quantum yields for **3** and **4** were 27% and 26%, respectively, and remained unchanged after replacement of the pyrazole ring with the phenyl group in **5** (26%). This observation was in line with our previous studies on heteroleptic pyridylarylboronic quinolinates, which showed very similar emission profiles and fluorescence quantum yields with respect to the Ph_2BQ reference complex.[19] On the other hand, the optical properties were affected by the type of aromatic linker between two boron centres. In the thiophene analogue **1**, the fluorescence quantum yield decreased to 22%, while compound **2** did not emit. We hypothesize that this may be due to the Photoinduced Electron Transfer effect which is characteristic for some nonplanar fluorescent molecules.[25]

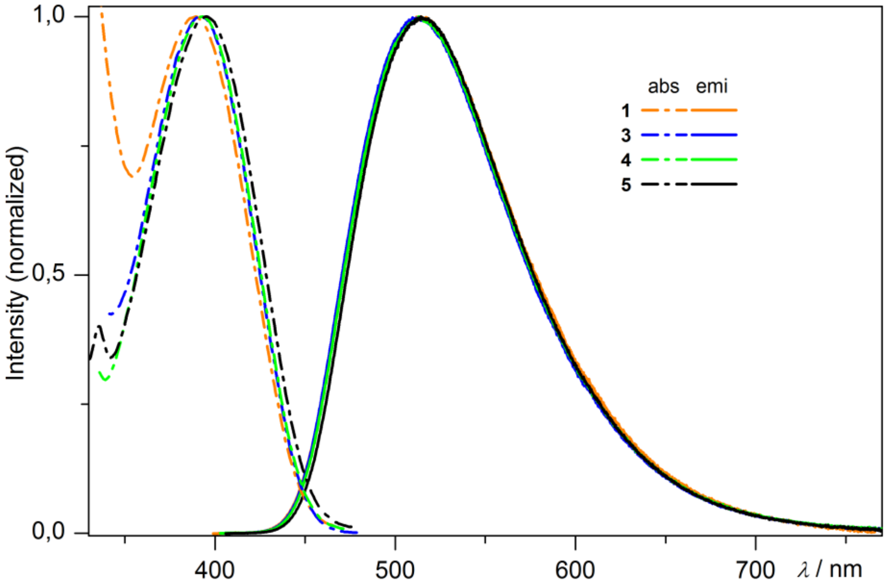

Figure 2. Normalized UV-Vis absorption and emission spectra of **1**, **3-5**. Full UV-Vis absorption spectrum is illustrated in the ESI Fig. S2.

Table1. Experimental and calculated photophysical properties of **1-5**

	Experimental					TD-DFT			
Compound	λ_{max} [nm]	ε [M^{-1} cm^{-1}]	λ_{em} [a] [nm]	Δ [cm^{-1}]	Φ [b] [%]	λ_{max} [nm]	*f*	λ_{em} [nm]	*f*
Ph_2BQ	396	-	504		23 [c] 30 [d]	-	-	-	-
1 [c]	389 316	1600 2400	515	6289	22	354	0.119	470	0.057
2 [c]	375 320	7600 22500	-	-	0	397	0.007	585	0.031
3 [d]	393	5500	513	5952	27	355	0.177	465	0.066
4 [c]	393	6200	513	5952	26	470	0.050	476	0.047
5 [c]	396	5500	514	5797	26	362	0.174	468	0.070

[a] All compounds were excited at the maximum of the longest wavelength absorption band.

[b] Standard coumarin 153 in EtOH ($c = 4.5 \cdot 10^{-6}$ mol·dm^{-3} in CH_2Cl_2)[26]

[c] CH_2Cl_2, [d]$CHCl_3$.

To understand the nature of electronic transitions in the studied molecules, experimental studies were supported with computational studies involving optimization of the ground state geometries for **1-5** at the M06-2X/6-31++g(d,p) level of theory. The optimized geometries were further utilized to examine the origin of electronic excitations by time-dependent density functional theory (TD-DFT). The calculated absorption and emission wavelengths are summarized in Table 1, while frontier molecular orbitals are shown in Figure 3. The TD-DFT calculations reproduce the spectroscopically obtained absorption and emission bands relatively well as the differences typically did not exceed 10%.

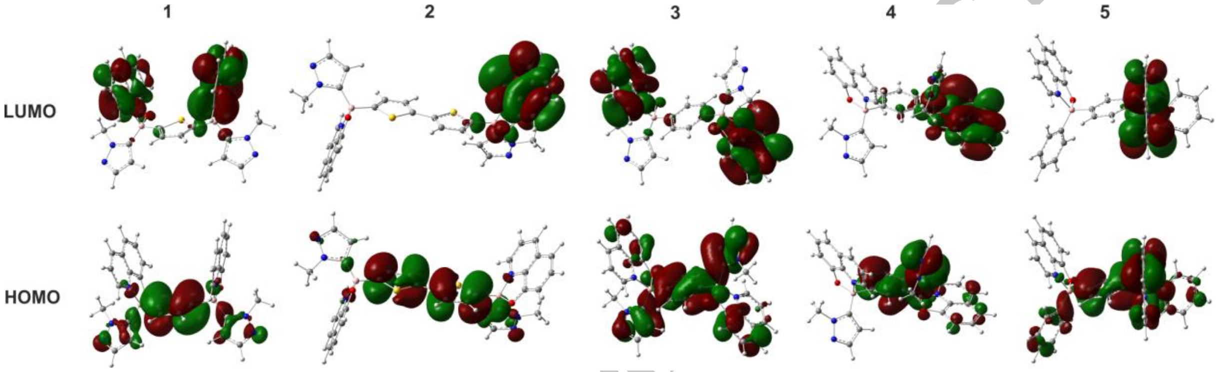

Figure 3.The HOMO and LUMO orbitals generated for compounds **1-5**. All orbitals from HOMO-4 to LUMO+4 are illustrated in the ESI (Fig. S3-S7).

The HOMO in compounds **1** and **2** is delocalized over the thiophene linker with small contributions from the pyrazole rings (Fig. 3). In turn, the BQ moieties contribute to the deeper molecular orbitals (HOMO-4–HOMO-1). In the cases of compounds **3** and **4**, the HOMO is spread over the phenyl linker and two pyrazole rings with some contribution from the BQ units. For these compounds the HOMO-1 and HOMO-2 are mostly located on the BQ moieties. In compound **5**, the HOMO is spread over the entire molecule except one BQ segment, which in turn, contributes to the HOMO-1 orbital. For all complexes the first four virtual orbitals are located mostly on the BQ moiety with no contributions from the pyrazole fragments or aromatic linker. In the case of **1** and **3** the LUMO is distributed equally over the two BQ units, whereas in **2**, **4** and **5** it is located on one of the BQ units with the energetically related LUMO+1 resides on the other.

Taking into account the location of frontier orbitals, the HOMO to LUMO transition occurs from the aromatic linker to the BQ moiety. However, since the frontier orbitals are located in different parts of the molecule, such transitions may be less efficient. This is especially noticeable for complexes **1-2**, where the energy of the HOMO orbital is elevated with respect to **3-5** (ESI, Table S1) and it is completely separated from the LUMO orbital by two boron centres. The stronger absorption peak for these two complexes appears at *ca*. 320 nm and can be attributed to electronic transition from the inner molecular orbitals (HOMO-1 and deeper), which are mostly located on the same segment as the LUMO.

Cyclic voltammetry (CV) studies of **1**–**5** were performed in order to establish their electrochemical redox properties in an organic solvent (CH_3CN, CH_2Cl_2). Potentials were assigned versus the ferrocene−ferrocenium ($FeCp_2/FeCp_2^+$) redox couple (Table 2) and the CV curves are depicted in ESI, Fig. S8. For compound **3** an irreversible oxidation wave was observed, whereas **1**, **2**, **4** and **5** displayed a quasi-reversible oxidation couple. Differences attributable to the substitution pattern and nature of linker were also observed. Complexes **1** and **2** containing an electron rich thiophene linker possessed lower oxidation potentials than compounds **3-5** containing a phenyl linker. The difference in oxidation and reduction potentials in **3** and **4** is mainly due to the auxiliary chromophoric effect which depends on the position of substituents in the phenyl linker. The HOMO and LUMO energy values for **1-5** were determined based on the corresponding peak potentials. The band gap obtained for **4** corresponds with the measured excitation energy, suggesting the pure HOMO-LUMO transition for this compound. However, for compounds **1-3** and **5** the band gaps obtained from the CV curves were lower than the measured excitation energy suggesting the electronic transition from inner molecular orbitals (HOMO-1 and deeper).

Table 2. Electrochemical data and calculated HOMO-LUMO energies for **1-5**.

Compound	E_{ox} [V]^a	E_{red} [V]^a	HOMO [eV]	HOMO-1 [eV]	LUMO [eV]	LUMO+1 [eV]	Bandgap [eV]
1	0.43; 1.74	-0.94; -1.90	-5.23	-6.54	-3.86	-2.90	1.37
2	0.44; 1.47	-0.94; -1.94	-5.24	-6.27	-3.86	-2.86	1.38
3	1.43	-0.95; -2.02	-6.23		-3.85	-2.78	2.38
4	1.12; 1.19	-2.03	-5.92	-5.99	-2.77		3.15
5	1.12; 1.20	-0.97; -2.08	-5.92	-6.00	-3.83	-2.72	2.09

[a] Values calculated on the basis of peak potentials with respect to the $FeCp_2/FeCp_2^+$ redox pair.

Conclusion

We have developed a one-pot synthetic approach to a novel class of heteroleptic bis(1-methyl-1*H*-pyrazole-5-yl)aryldiborinic-bis(8-oxyquinolinates) bearing two pyrazole moieties bonded to the boron atoms and central units built from the benzene, thiophene or bithiophene ring. The fluorescent properties of complexes **1** and **3**–**5** exhibited emission at *c.a.* 513 nm and moderate quantum yields in the range of 22-27 %. Thiophene based complex **1** exhibited the lowest quantum yield, whereas no emission was observed for bithiophene derivative **2**. Based on the results of TD-M06-2X/6-31++g(d,p) calculations, the longest absorption wavelength comes from the HOMO to LUMO transition and can be attributed to charge migration from the aromatic linker to the BQ ligand. However, the efficiency of this transition may vary depending on aromatic group linking two boron centres. The obtained complexes **2-4** show improved thermal stability with respect to their phenyl analogue **5**. Furthermore, implementation of the pyrazole moiety into the complex scaffold greatly improved the solubility of the compounds. Therefore, it can be proposed that the use of pyrazole-based organoboron complexes would be beneficial from the perspective of application in photoluminescent devices. It is also plausible that **1** and **3-5** can be used as building blocks in the construction of various supramolecular luminescent systems.

Acknowledgments: This work was supported by the National Science Centre (Narodowe Centrum Nauki, Grant No. 2015/19/D/ST5/00735) and by the Warsaw University of Technology. The X-ray measurements of compounds **1** and **3** were undertaken at the Crystallographic Unit of the Physical Chemistry Laboratory, Chemistry Department, University of Warsaw. Support from Aldrich Chemical Company, Milwaukee, WI, USA, through the donation of chemicals and equipment is gratefully acknowledged.

References

---

1. Mukherjee, S.; Thilagar, P. *J. Mater. Chem. C* **2016**, *4*, 2647.
2. Mukherjee, S.; Thilagar, P. *Chem. Commun.* **2015**, *51*, 10988.
3. Wesela-Bauman, G.; Urban. M.; Luliński, S.; Serwatowski, J.; Woźniak, K. *Org. Biomol. Chem.* **2015**, *13*, 3268.
4. Frath, D.; Massue, J.; Ulrich, G.; Ziessel, R. *Angew. Chem., Int. Ed.* **2014**, *53*, 2290.
5. Wesela-Bauman, G.; Luliński, S.; Serwatowski, J.; Woźniak, K. *Phys. Chem. Chem. Phys.* **2014**, *16*, 22762.
6. Li, D.; Zhang, H.; Wang, Y. *Chem. Soc. Rev*. **2013**, *42*, 8416.
7. Cheng, F.; Bonder, E.; Salem, S.; Jäkle, F. *Macromolecules* **2013**, *46*, 2905.
8. Tanaka, K.; Chujo, Y. *Macromol. Rapid Commun*. **2012**, *33*, 1235.
9. Rao, Y. -L.; Wang, S. *Inorg. Chem*. **2011**, *50*, 12263.
10. Jäkle, F. *Chem. Rev*. **2010**, *110*, 3985.
11. Tokoro, Y.; Nagai, A.; Chujo, Y. *Appl. Organomet. Chem.* **2010**, *24*, 563.
12. Tokoro, Y.; Nagai, A.; Kokado, K.; Chujo, Y. *Macromolecules* **2009**, *42*, 2988.
13. Hellstrom, S. L.; Ugolotti, J.; Britovsek, G. J. P.; Jones, T. S.; White, A. J. P. *New J. Chem.* **2008**, *32*, 1379.
14. Qin, Y.; Kiburu, I.; Shah, S.; Jäkle, F. *Org. Lett.* **2006**, *8*, 5227.
15. Kappaun, S.; Rentenberger, S.; Pogantsch, A.; Zojer, E.; Mereiter, K.; Trimmel, G.; Saf, R.; Möller, K. C.; Stelzer, F.; Slugovc, C. *Chem. Mater.* **2006**, *18*, 3539.
16. Cui, Y.; Wang, S. *J. Org. Chem.* **2006**, *71*, 6485.
17. Cui, Y.; Liu, Q. –D.; Bai, D. -R.; Jia, W.-L.; Tao, Y.; Wang, S. *Inorg. Chem.* **2005**, *44*, 601.

---

18. Wang, X. Y.; Weck, M. *Macromolecules* **2005**, *38*, 7219.

19. Wesela-Bauman, G.; Ciećwierz, P.; Durka, K.; Luliński, S.; Serwatowski, J.; Woźniak, K. *Inorg. Chem.* **2013**, *52*, 10846.

20. Durka, K.; Głowacki, I.; Luliński, S.; Wiosna-Sałyga, G.; Woźniak, K. *J. Mater. Chem. C* **2015**, *3*, 1354.

21. See references 6, 19 and 20.

22. Nöth, H.; Regnet, W.; Riehl, H.; Standfest, R. *Chem. Ber*. **1971**, *104*, 722.

23. Zhao, Y.; Truhlar, D. *Theor. Chem. Acc.* **2008**, *120*, 215.

24. Cui, Y.; Liu, Q. D.; Bai, D. R.; Jia, W. L.; Tao, Y.; Wang, S. *Inorg. Chem.* **2005**, *44*, 601.

25. Loudet, A.; Burgess, K. *Chem. Rev*. **2007**, *107*, 4891.

26. Brouwer, A. M. *Pure Appl. Chem*. **2011**, *83*, 2213.

Highlights

The obtained pyrazole-based complexes show high solubility and thermal stability

Complexes exhibit emission *c.a.* 513 nm with quantum yields of 22-27%

Complexes can be obtained using a simple one-pot protocol